Comparison of the Average-t-Matrix and Coherent-Potential Approximations in Substitutional Alloys*

L. Schwartz, F. Brouers,† A. V. Vedyayev,‡ and H. Ehrenreich
Division of Engineering and Applied Physics, Harvard University, Cambridge, Massachusetts 02138
(Received 11 June 1971)

This paper will review techniques useful in theoretical analyses of the electronic structure of disordered substitutional alloys. The coherent-potential approximation (CPA) and the average-t-matrix approximation (ATA), which have received a great deal of attention recently, are compared for two model Hamiltonians. A reconsideration of the ATA shows that the unphysical results usually attributed to it are in fact the consequence of unnecessary further approximations. The two Hamiltonians in question consist, respectively, of a single-band model and a two-band model relevant to the description of transition-metal alloys. In the first case the ATA is found to provide a correct description of the qualitative features of the density of states for a wide variety of scattering strengths and concentrations. In the two-band model, which has been previously applied in connection with the optical properties of Ag-Au alloys, the results of the ATA and the CPA are essentially identical over a wide range of energies. This agreement can be shown to persist as long as the constituent d subbands lie within the broad s band of the alloy. This is precisely the situation that obtains in many of the transition- and noble-metal alloys. This result is of particular importance since the ATA is far easier to implement numerically than the CPA. In fact, the ATA may be regarded as a good first approximation in an iteration scheme leading to the self-consistent CPA solution.

I. INTRODUCTION

This paper is concerned with the single-particle theory of the electronic structure of disordered binary alloys. This problem has generally been discussed within the framework of multiple-scattering theory.[1-9] Such a procedure is appropriate if the disordered potential of the alloy can be decomposed into a sum of contributions due to the individual atomic scatterers. The propagation of an electron through the system may then be viewed as a succession of elementary scatterings from these random atomic potentials.

Recently, several authors[7-9] have emphasized the importance of treating these multiple-scattering events self-consistently. In this approach the scatterers are viewed as being embedded in an effective medium whose choice is open. The choice is made self-consistently by requiring that the average scattering from a single ion be set equal to zero. The effective medium corresponding to this choice is usually referred to as the coherent-potential medium.

In practice, the implementation of the coherent-potential approximation (CPA) requires the calculation of the full Green's function $G(z)$ for the periodic effective medium. In a realistic solid this is a formidable task involving the evaluation of complicated integrals over the Brillouin zone. Consequently the application of the CPA has been limited to model Hamiltonians with a relatively small number of input parameters.[7-12]

It is the purpose of the present paper to reconsider an alternative approach to the calculation of the electronic density of states in disordered alloys. This method, the average-t-matrix approximation (ATA), which predates the CPA, does not require a self-consistent procedure. Its name derives from the fact that the effective medium is determined by simply requiring that it reproduce the average scattering at each site. The utility of the ATA has not been fully explored because in the past, several authors[4-6] have argued that it leads to unphysical results for the density of states. In particular, the existence of spurious gaps[5] in $\rho(E)$ has often been associated with the ATA. It will be seen that these difficulties are not really inherent in the ATA but are instead the consequence of several unjustified further approximations. A similar situation exists in the theory of systems with structural rather than compositional disorder.[1,13-16] In liquid metals, for example, the quasicrystalline[13,14] approximation, which is the direct analog of the ATA,[16] is known to be a useful first approximation.

To demonstrate that the ATA is a viable method in the alloy problem, numerical calculations are presented for two of the model Hamiltonians for which the results of the CPA are readily available. The simplest of these, the single-band model of Velický, Kirkpatrick, and Ehrenreich[8] (VKE) and Soven,[9] is discussed in Sec. II. It is shown that the ATA does in fact provide a reasonable description of the density of states over the entire range of scattering strengths and that for moderate

strengths the results of the CPA and ATA are essentially identical. In Sec. III we consider a two-band Hamiltonian capable of describing the basic features of the transition- and noble-metal alloys. The model is a slightly generalized version of the one used by Levin and Ehrenreich[12] to discuss the concentration dependence of the optical absorption edge in Au-Ag. Adopting their parameters, we are able to compare the ATA and CPA for the Au-Ag system. The agreement between the two methods is remarkably good. Indeed, in the dilute limit (concentration ~ 10%) the results are essentially identical.

On the basis of these preliminary findings, we conclude that the importance of non-self-consistent methods in the alloy problem has been seriously underestimated. While it remains true that the CPA is the best of all single-site approximations, its formal complexity may well limit its application to simple model Hamiltonians. By contrast, the relative simplicity of the ATA may make it a more useful technique for the descriptions of realistic systems.

II. SINGLE-SITE APPROXIMATIONS AND SINGLE-BAND MODEL

This section begins with a review of the formalism underlying the single-site description of binary alloys. The coherent-potential and average-t-matrix approximations are then introduced as alternative versions of the single-site approximation. For convenience this discussion is limited to the single-band model.[8,9]

Consider the alloy to be described in a tight-binding representation. A single orbital $|n\rangle$ is associated with each site n. The one-electron Hamiltonian is

$$H=\sum_n |n\rangle \epsilon_n^{A(B)} \langle n| + \sum_{n\neq m} |n\rangle h_{nm} \langle m| \tag{1}$$

$$= D + W . \tag{2}$$

The second line defines the separation of H into a diagonal part D and an off-diagonal part W. The diagonal elements may be regarded as random atomic levels which assume one of two possible values ϵ^A or ϵ^B depending on whether an atom of type A or B occupies the site n. The respective concentrations of A and B atoms are x and $y \equiv 1-x$, both varying between 0 and 1. The hopping integrals h_{nm} are assumed to be independent of the alloy configuration. The operator W may therefore be interpreted as the Hamiltonian of the pure crystal for which $\epsilon^A = \epsilon^B = 0$.

The matrix elements of W in the Bloch representation are given by

$$\langle k \mid W \mid k' \rangle = \delta_{kk'} w\, s(k). \tag{3}$$

$s(k)$ describes the k dependence of the band energy and w is one-half the band-width. It is convenient to express ϵ^A and ϵ^B in terms of w to define the zero of energy such that

$$\epsilon^A = \tfrac{1}{2} w\delta = -\epsilon^B .$$

This equation defines the dimensionless impurity strength δ. The energy w simply scales the entire Hamiltonian and will be set equal to unity. For a given choice of W, the alloy is completely specified by the two parameters x and δ characterizing, respectively, the concentration and separation of the energy bands.

The equilibrium properties of the alloy are discussed most simply in terms of the Green's function

$$G(z) = (z - H)^{-1}. \tag{4}$$

In particular, the ensemble average of $G(z)$, to be denoted by $\langle\langle G(z)\rangle\rangle$, determines all the macroscopic properties of interest in the one-electron approximation. $\langle G \rangle$ may be used to define a self-energy $\Sigma(z)$,

$$\langle G(z)\rangle = [z - W - \Sigma(z)]^{-1}. \tag{5}$$

$\Sigma(z)$ has the symmetry of the lattice but will in general be complex and non-Hermitian. Because the average alloy is characterized by the effective medium described by Σ, it is often convenient to rewrite H in the form

$$H = W + \sum_n |n\rangle \sigma(z) \langle n| + \sum_n |n\rangle [\epsilon_n^{A(B)} - \sigma(z)] \langle n|$$

$$\equiv \tilde{H} + \sum_n |n\rangle [\epsilon_n^{A(B)} - \sigma(z)] \langle n| \tag{6}$$

$$\equiv \tilde{H} + \sum_n |n\rangle v_n \langle n| . \tag{7}$$

v_n then describes scattering relative to a reference Hamiltonian $\tilde{H}$ which may be chosen at will. It will be seen that better choices for $\sigma(z)$ lead to successively better approximations to $\langle G(z)\rangle$.

The calculation of $\langle G \rangle$ is carried out most easily within the framework of multiple-scattering theory. For a given configuration of the alloy, the relation between G and the total scattering operator T is simply

$$G = \tilde{G} + \tilde{G}\, T \tilde{G} . \tag{8}$$

Here

$$\tilde{G}(z) \equiv (z - \tilde{H})^{-1} = G^{(0)}(z - \sigma(z)) \tag{9}$$

is the reference propagator and $G^{(0)}(z) \equiv (z - W)^{-1}$ is the Green's function for the perfect crystal with Hamiltonian W. Equations (4), (6), and (8) may be used to express T in terms of t_n, the scattering matrix for the nth ion,

$$t_n = |n\rangle \frac{v_n}{1 - v_n \tilde{F}(z)} \langle n| , \tag{10}$$

where $\tilde{F}(z) \equiv \langle n | \tilde{G}(z) | n \rangle$. The result is simply[8,9]

$$T = \sum_n T_n , \tag{11}$$

$$T_n = t_n \left(1 + \tilde{G} \sum_{m \neq n} T_m \right) . \tag{12}$$

Iteration of (12) leads to the usual multiple-scattering expansion[3,6]

$$T_n = t_n + t_n \tilde{G} \sum_{m \neq n} t_m + t_n \tilde{G} \sum_{m \neq n} t_m \tilde{G} \sum_{p \neq m} t_p + \cdots . \tag{13}$$

Equations (8)–(13) are exact. They lead to the exact averaged relations

$$\langle T \rangle = \sum_n \langle T_n \rangle , \tag{14}$$

$$\langle T_n \rangle = \langle t_n \rangle \left(1 + \tilde{G} \sum_{m \neq n} \langle T_m \rangle \right) + \left\langle (t_n - \langle t_n \rangle) \tilde{G} \sum_{m \neq n} (T_m - \langle T_m \rangle) \right\rangle . \tag{15}$$

The first term in (15) may be thought of as describing the average effective wave seen by the nth ion, while the second term describes fluctuations in the effective wave. Our basic approximation, to be referred to as the single-site approximation,[8] is the neglect of this difficult term. The electronic properties of the alloy are then determined from the closed set of equations

$$\langle T_n \rangle = \langle t_n \rangle \left(1 + \tilde{G} \sum_{m \neq n} \langle T_m \rangle \right) . \tag{16}$$

Using the fact that $\sum_{m \neq n} T_m = T - T_n$, Eq. (16) is easily rewritten as

$$\langle T_n \rangle = [1 + \tilde{F} \langle t_n \rangle]^{-1} \langle t_n \rangle [1 + \tilde{G} \langle T \rangle] .$$

Combining this result with (8) and (5), we obtain

$$\Sigma(z) = \sigma(z) + \frac{\langle t \rangle}{1 + \langle t \rangle \tilde{F}(z)} . \tag{17}$$

This equation can be used in two ways. Either $\langle t \rangle$ and $\tilde{F}$ corresponding to a given choice of $\sigma(z)$ can be inserted into (17) or the equation

$$\langle t \rangle = 0 \tag{18}$$

may be used to determine $\sigma(z)$. In the second case Eq. (17) guarantees that $\langle G \rangle = \tilde{G}$ since $\Sigma(z) = \sigma(z)$. These two possibilities define two different classes of approximate calculations of $\Sigma(z)$ within the single-site approximation. In the first case, the second term in (17) describes an effective potential corresponding to the average scattering matrix at the site n. Accordingly, this method is known as the average-t-matrix approximation (ATA).[3–6] The second approach, usually referred to as the coherent-potential approximation (CPA)[7–9] requires a self-consistent solution of (18) and is much more difficult to implement numerically than the ATA.

Substituting from (7) and (10) into (18), we see that within the single-band model, the coherent-potential equation may be written as

$$0 = \frac{x(\epsilon^A - \Sigma)}{1 - (\epsilon^A - \Sigma)\tilde{F}(z)} + \frac{y(\epsilon^B - \Sigma)}{1 - (\epsilon^B - \Sigma)\tilde{F}(z)}$$

or, more simply,

$$\Sigma(z) = \epsilon + \frac{xy\delta^2 \tilde{F}(z)}{1 + [\epsilon + \Sigma(z)]\tilde{F}(z)} , \tag{19}$$

where $\epsilon = x\epsilon^A + y\epsilon^B = \frac{1}{2}(x - y)\delta$. Equation (19) must be solved self-consistently for $\Sigma(z)$ and $\tilde{F}(z) = F^{(0)}(z - \Sigma(z))$. The details of such a procedure have been discussed by Soven[9] and VKE.[8] These authors have shown that the CPA provides a reasonable description of the alloy over a wide range of the parameters x and δ.

Consider now the ATA for the single-band model. Because this approach is not self-consistent, the results will in general depend on the choice of $\tilde{H}$. Suppose, for example, that we take $\tilde{H}$ to be the virtual-crystal Hamiltonian, i.e., $\sigma(z) = \epsilon$. Equations (7), (10), and (17) then give

$$\Sigma(z) = \epsilon + \frac{xy\delta^2 F^{(0)}(z - \epsilon)}{1 + 2\epsilon F^{(0)}(z - \epsilon)} . \tag{20}$$

The density of states in the ATA is obtained by substituting from (20) into the usual formula

$$\rho(E) = -\pi^{-1} \operatorname{Im} F^{(0)}(z - \Sigma(z)) \Big|_{z = E^+} . \tag{21}$$

It will be seen shortly that Eqs. (20) and (21) are capable of describing many of the qualitative features of the electronic structure in the alloy. The form of (20) is quite similar to that of the CPA equation. The ATA may in fact be viewed as the first iteration [i.e., $\Sigma(z) \to \epsilon$] of Eq. (19) toward self-consistency. It is interesting to note that in the virtual-crystal regime, i.e., $\delta \ll 1$, the CPA and ATA agree to $O(\delta^2)$:

$$\Sigma(z) = \epsilon + xy\delta^2 F^{(0)}(z - \epsilon) .$$

The denominators in (19) and (20) have been neglected because $2\epsilon = (x - y)\delta$ is $O(\delta)$.

Several authors[3,6] have argued that the non-self-consistent ATA does not yield correctly even the simplest features of the electronic structure of binary alloys. In particular, the existence of spurious gaps in the density of states has generally been associated with this method. It is the purpose of this paper to show that these difficulties are not inherent in the ATA but are rather a consequence of the improper implementation of that method. Equations (20) and (21) allow us to understand how

spurious gaps in $\rho(E)$ may appear if the ATA is treated incorrectly. If the replacement $F^{(0)}(z) \to 1/z$ (appropriate only in "atomic limit" $\delta \to \infty$ as $w \to 0$)[8] is made, we obtain

$$\Sigma(z) = \epsilon + xy\delta^2/(z+\epsilon) . \tag{22}$$

This expression for $\Sigma(z)$ is singular at $z = -\epsilon$, and consequently leads to a gap in $\rho(E)$ at this energy. Such behavior is reasonable in the atomic limit where the spectrum consists of two well-separated atomic levels centered at ϵ^A and ϵ^B, but is entirely spurious if (22) is applied to the regime $\delta \lesssim 1$.

Previous authors[3,6] have discussed the ATA from an alternative point of view. Rather than introducing a self-energy operator, they view (16) as a prescription for the calculation of $\langle T_n \rangle$. Most often this equation is written in the form

$$\langle T_n \rangle = \langle t_n \rangle + \langle t_n \rangle \tilde{G} \sum_{m \neq n} \langle t_m \rangle + \langle t_n \rangle \tilde{G} \sum_{m \neq n} \langle t_m \rangle \tilde{G} \sum_{p \neq m} \langle t_p \rangle + \cdots . \tag{23}$$

If (23) is combined with (14) and (8), an expression for $\langle G(z) \rangle$ is obtained directly. It can be shown that the density of states implied by this procedure is indeed equivalent to that of Eqs. (20) and (21). The algebra required to make this connection is somewhat tedious and will be discussed in the Appendix. When this approach to the ATA is employed, the unphysical gaps in $\rho(E)$ may be traced to the assumption[17]

$$t^{A(B)} \simeq (E - \epsilon^{A(B)})^{-1} .$$

Equation (10) shows that this approximation is valid only if E is well outside the unperturbed band so that $F^{(0)}(z) \simeq 1/z$. Once again, the spurious features in $\rho(E)$ are associated with the improper use of the atomic limit.

Within the single-band model, it is useful to compare the results of a given approximate method (for example, the ATA and CPA) with exact results concerning the sum rules and moments of various physical quantities. The simplest such quantity is the density of states $\rho(E)$ whose moments are defined by

$$\mu_p = \int_{-\infty}^{\infty} E^p \rho(E)\, dE .$$

If p is small, a procedure developed by VKE may be used to calculate the moments μ_p exactly. It can then be shown that the ATA and CPA lead to densities of states that give correct values for the first four and seven moments, respectively. In this context it is quite clear that the results of the ATA depend on the choice of $\tilde{H}$. If, instead of $\sigma = \epsilon$, we had made the simpler choice $\sigma = 0$ (i.e., $\tilde{H} = W$), then only the first three of the ATA moments would have been exact. As with any non-self-consistent perturbation procedure, the ATA may be improved if a careful starting point is employed.

Equations (19) and (20) show that the implementation of the ATA and CPA requires only the calculation of $F^{(0)}(z)$. Using the relation

$$F^{(0)}(z) = \int_{-\infty}^{\infty} \frac{\rho^{(0)}(E)}{z - E}\, dE , \tag{24}$$

we see that x, δ, and $\rho^{(0)}(E)$ completely define the alloy problem within the single-site approximation.

Following VKE, we assume that $\rho^{(0)}(E)$ has the form suggested by Hubbard,

$$\rho^{(0)}(E) = (2/\pi w^2)\,(w^2 - E^2)^{1/2}, \quad |E| < w$$
$$= 0, \quad |E| > w .$$

$F^{(0)}(z)$ is then simply

$$F^{(0)}(z) = (2/w^2)\,[z - (z^2 - w^2)^{1/2}] .$$

The results for the density of states in three cases is shown in Fig. 1. We see that both the ATA and CPA exhibit the development for increasing δ, of the band shape from the virtual-crystal regime through a stage where the band is distorted at its upper edge until it finally splits into independent subbands. These figures provide a corrected version of VKE's Fig. 3(c). The ATA calculation described in Ref. 8 was actually based on Eq. (22) [their (4.21)] and consequently exhibited a gap in $\rho(E)$ for all values of δ. The ATA and CPA are now seen to be qualitatively similar over the entire range of δ.

A more detailed comparison shows that, while the location and weights of the subbands are given correctly by both methods, the CPA describes their shape more correctly. In particular, the height and width of the CPA minority band both vary as $\sqrt{x}$, while in the ATA they vary as 1 and x, respectively. This difference is a reflection of the fact that four subband moments are given exactly in the CPA, while only two are exact in the ATA. The self-consistency of the CPA improves not only the general shape of $\rho(E)$ as indicated by the moments, but also various finer structural details. In Fig. 1(a) the sharp cusp in the upper edge of the ATA density of states is a spurious effect due to the fact that non-self-consistent theories allow quasiparticles to decay into bare-particle states. This point has been discussed by VKE in connection with their Fig. 2. We see also that the ATA majority bands in Fig. 1(b) and 1(c) exhibit a residual "tail" at their upper edges. This tail is associated with the fact that $\Sigma(z)$ in (20) is calculated in terms of $F^{(0)}(z - \epsilon)$. Consequently $\mathrm{Im}\Sigma(E^+)$ and therefore $\rho(E)$ must be

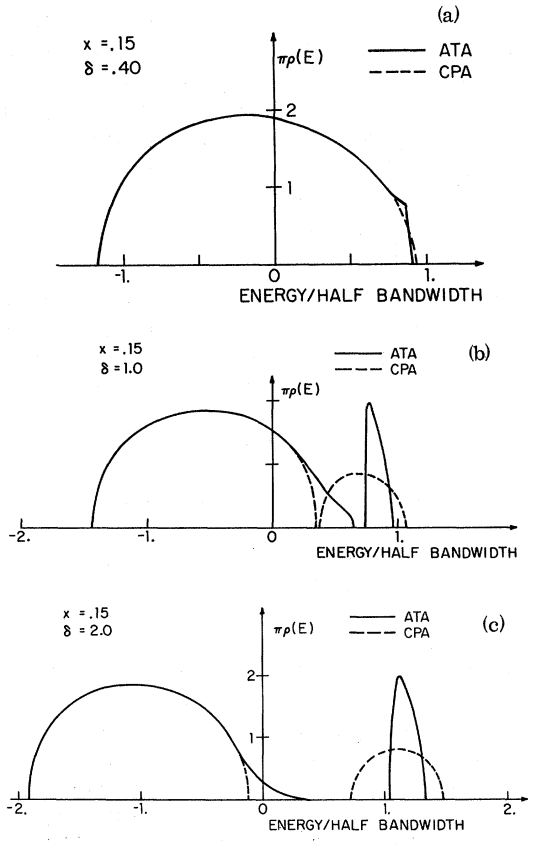

FIG. 1. Comparison of the density of states calculated in the coherent-potential and average-t-matrix approximations. In each case $x = 0.15$; the values of δ are 0.4, 1.0, and 2.0.

finite in the energy range $|z - \epsilon| \leq 1$.

These apparent drawbacks of the ATA are actually overemphasized by the single-band model. In the following section it will be seen that for another type of model Hamiltonian appropriate to the transition metals, the agreement between the ATA and CPA is greatly improved.

III. TWO-BAND MODEL: Au-Ag ALLOYS

In this section we discuss a two-band model for the noble- and transition-metal alloys. The model is a generalized version of the one used by Levin and Ehrenreich[12] (LE) to describe the optical absorption edge in Au-Ag alloys. Adopting parameters appropriate to silver and gold, the model is used to compare the ATA and CPA. It will be seen that the densities of states predicted by the two methods are in good agreement over the entire range of energies considered. In Sec. II it was shown that the difference between the ATA and CPA is negligible if the single-band parameter δ is small. We conclude this section by discussing the range of parameters for the two-band model over which the CPA and ATA are expected to agree.

The pure metals A and B are assumed to have a broad s band and a narrow d band centered at the energy $\epsilon_d^{A(B)}$. The d band is supposed to consist of five degenerate but independent subbands. In the model discussed by LE the d band was replaced by a single level of zero width. This assumption tends to overemphasize the effects of s-d hybridization and leads to the appearance of unphysical hybridization gaps in the density of states for the pure metals. The introduction of a width in the d band eliminates this difficulty.

In the alloy A_xB_{1-x} the d energy level at a given site may be ϵ_d^A or ϵ_d^B. The disorder associated with these random d levels will be treated in the ATA and the CPA. By contrast, the s-band and hybridization parameters are assumed to exhibit virtual-crystal behavior. For a given configuration of the alloy, the Hamiltonian is

$$H = \sum_{k\in BZ} E_s(k)\,|k_s\rangle\langle k_s| + \sum_{k\in BZ} \epsilon_d(k)\,|k_d\rangle\langle k_d| + \sum_n \epsilon_d^{A(B)}\,|n_d\rangle\langle n_d| + \sum_{k\in BZ} \bar{\gamma}\,[\,|k_s\rangle\langle k_d| + |k_d\rangle\langle k_s|\,]\,. \quad (25)$$

The first two terms represent the kinetic energy of the s and d electrons. The third term contains the random d levels and the last terms describe the s-d hybridization. The intersection of the $E_s(k)$ curve with the (spherical) Brillouin-zone boundary determines the width $2w_s$ of the unhybridized s band:

$$E_s(k) = E_0^{A(B)} + w_s s(k). \quad (26)$$

For a given metal, the parameters $E_0^{A(B)}$, w_s, ϵ_d, and $\gamma(\epsilon_d)$ may be chosen to fit existing band calculations approximately. The relevant procedure has been discussed in detail by LE and need not be repeated here. As indicated above, the s-band and hybridization parameters in the alloy are assumed to satisfy

$$E_0 \to \bar{E} = xE_0^A + yE_0^B\,, \quad (27a)$$

$$\gamma \to \bar{\gamma} = x\gamma(\epsilon_d^A) + y\gamma(\epsilon_d^B)\,. \quad (27b)$$

In addition, it is convenient to suppose that in a given metal the unhybridized s and d bands have the same shape but differ in location and width. If the energy origin is chosen midway between the constituent d levels, we have

$$E_s(k) = \bar{E} + w_s s(k)\,, \quad (28a)$$

$$\epsilon_d(k) = \alpha w_s s(k)\,. \quad (28b)$$

The parameter α, which specifies the relative

width of the s and d bands, is a new feature of the present model. In practice, we choose a value of α that is large enough to eliminate the hybridization gap ($\alpha \sim 3\gamma^2$) but otherwise leaves the density of states unchanged.

The third term of (25) is the only part of the Hamiltonian to be treated on the basis of the CPA or ATA. It is in fact identical to the corresponding term of the single-band Hamiltonian. Because of this similarity, ATA and CPA calculations for the two-band model are essentially no more difficult than those discussed in Sec. II.

In the present case, the propagator $\langle G(z)\rangle$ is a 2×2 matrix, which may be written in the $\{|k_s\rangle, |k_d\rangle\}$ representation as

$$\langle G(z)\rangle = \begin{bmatrix} z - E_s(k) & -\bar{\gamma} \\ -\bar{\gamma} & z - \epsilon_d(k) - \Sigma_d(z) \end{bmatrix}^{-1} . \quad (29)$$

The self-energy $\Sigma_d(z)$ is seen to enter only the d-d part of $\langle G\rangle$. As in Sec. II, the calculation of $\langle G\rangle$ is carried out most simply in terms of the total scattering operator T. In the $\{|n_s\rangle, |n_d\rangle\}$ representation the equations are

$$T = \begin{bmatrix} 0 & 0 \\ 0 & \sum_n T_n \end{bmatrix} \quad (30)$$

and

$$T_n = t_n^d \left[1 + \tilde{G} \sum_{m\neq n} T_m\right], \quad (31)$$

where once again $\tilde{G}$ is the reference propagator. Averaging Eq. (31) and decoupling as in (16), the CPA and ATA equations are found to be

$$\Sigma^{\mathrm{CPA}}(z) = \bar{\epsilon}_d + \frac{xy\,\Delta^2 F_{dd}(z, \Sigma_d)}{1 + (\bar{\epsilon}_d + \Sigma_d) F_{dd}(z, \Sigma_d)} \quad (32)$$

and

$$\Sigma^{\mathrm{ATA}}(z) = \bar{\epsilon}_d + \frac{xy\,\Delta^2 F_{dd}(z, \bar{\epsilon}_d)}{1 + 2\bar{\epsilon}_d F_{dd}(z, \bar{\epsilon}_d)} , \quad (33)$$

respectively. Here $\Delta = \epsilon_d^A - \epsilon_d^B$, $\bar{\epsilon}_d = x\epsilon_d^A + y\epsilon_d^B$, and F_{dd} is the d-d matrix element of $\langle \tilde{G}(z)\rangle$:

$$F_{dd}(z, \Sigma_d) = \langle n_d | \langle \tilde{G}(z)\rangle | n_d\rangle$$

$$= N^{-1} \sum_{k\in \mathrm{BZ}} \langle k_d | \langle \tilde{G}(z)\rangle | k_d\rangle$$

$$= N^{-1} \sum_{k\in \mathrm{BZ}} \{z - \Sigma_d - \epsilon_d(k) - \bar{\gamma}^2 [z - E_s(k)]^{-1}\}^{-1} . \quad (34)$$

Equations (32) and (33) are seen to be structurally identical to (19) and (20), their counterparts in the single-band model. The fact that $E_s(k)$ and $\epsilon_d(k)$ are defined in terms of the same $s(k)$ allows Eq. (34) to be rewritten as

$$F_{dd}(z, \Sigma_d) = [\alpha(E_1 - E_2)]^{-1} [(z - \bar{E} - E_1) F_s^{(0)}(E_1) - (z - \bar{E} - E_2) F_s^{(0)}(E_2)] , \quad (35)$$

where E_1 and E_2 are the roots of the equation

$$E^2 - [z - \bar{E} - (z - \Sigma_d)/\alpha] E - \gamma^2/\alpha = 0. \quad (36)$$

$F_s^{(0)}$ in (35) is related to the unhybridized s-band density of states by an equation like (24). As in Sec. II, we adopt the Hubbard model for $\rho_s^{(0)}$.

Once Eqs. (32) and (33) have been used to evaluate $\Sigma_d(z)$, the density of states for the ten d electrons is obtained from the formula

$$\rho_d(E) = -(10/\pi)\,\mathrm{Im} F_{dd}(E^+, \Sigma_d) . \quad (37)$$

Similarly, the s-band contribution is given by

$$\rho_s(E) = -\pi^{-1}\,\mathrm{Im} F_{ss}(E^+, \Sigma_d)$$

$$= -\pi^{-1}\,\mathrm{Im}\langle n_s | \langle G(z)\rangle | n_s\rangle ,$$

where the relation between F_{ss} and $F_s^{(0)}$ is

$$F_{ss}(z, \Sigma_d) = (E_2 - E_1)^{-1} \{[(z - \Sigma_d)/\alpha - E_1] F_s^{(0)}(E_1) - [(z - \Sigma_d)/\alpha - E_2] F_s^{(0)}(E_2)\} .$$

To compare the ATA and CPA we have calculated the density of states for Au-Ag alloys of various concentrations. We use the same physical parameters quoted by LE, the only new feature of the present calculation being the intrinsic d bandwidth αw_s. Figure 2 shows the s and d density of states for the pure metals silver and gold. It is seen that the spurious d-band structure, evident in Fig. 2 of Ref. 12, is no longer present.

The d-band density of states obtained from the ATA and CPA is shown in Fig. 3. The first and last of these figures demonstrate that for dilute alloys the two methods yield essentially the same results. In both instances values of α appropriate to the host metal have been used. In the equiconcentration case [Fig. 3(b)] the ATA and CPA results differ in the energy region between the two subbands. The structure in the ATA density of states near $E = 0$ is spurious and may be traced to the unphysical hybridization gap that exists when $\alpha = 0$. It can be shown that this structure becomes less pronounced if α is increased slightly. In any event, within the present model Hamiltonian, the ATA is certainly capable of describing the essential features of the electronic density of states in Au-Ag alloys over the entire range of concentrations and energies. In addition, it should be emphasized that any experimental quantity that is independent of the

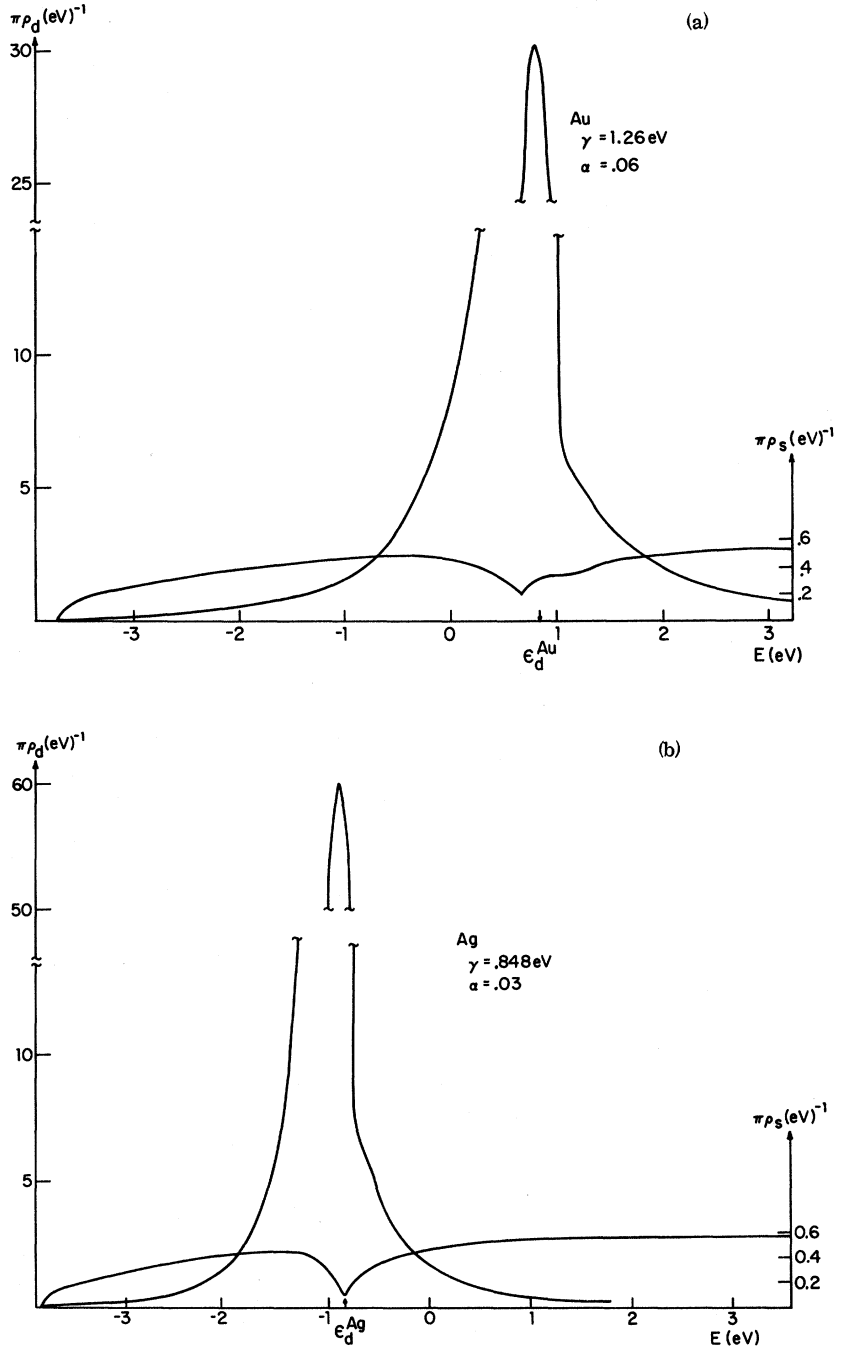

FIG. 2. Density of states for s and d bands for (a) Au and (b) Ag. Here, as in Fig. 3, the energy origin and the physical parameters are the same as in Figs. 2 and 3 of Ref. 12. The scaling factor α characterizing the width of the d band is equal to 0.06 for Au and 0.03 for Ag.

detailed shape of the d bands—for example, the shift of the optical absorption edge with concentration—could just as well be calculated from the ATA as the CPA.

These results for Au-Ag alloys suggest that it is possible to determine a range of parameters for the two-band model within which the ATA and CPA will agree. Because it is the first iteration of the CPA towards self-consistency, the ATA will be a good approximation if the right-hand side of (32) is relatively insensitive to small variations of Σ_d away from the value $\Sigma_d = \bar{\epsilon}_d$. We are essentially viewing (33) as the first of a Taylor expansion of Σ^{CPA}. The corrections are then given by

$$D(z) \equiv (\Sigma^{\mathrm{CPA}} - \Sigma^{\mathrm{ATA}})/(\Sigma^{\mathrm{CPA}} - \bar{\epsilon}_d)$$

$$\simeq \frac{d}{d\Sigma_d}\left[\frac{xy\Delta^2 F_{dd}(z, \Sigma_d)}{1 + (\bar{\epsilon}_d + \Sigma_d) F_{dd}(z, \Sigma_d)}\right]_{\Sigma_d = \bar{\epsilon}_d}$$

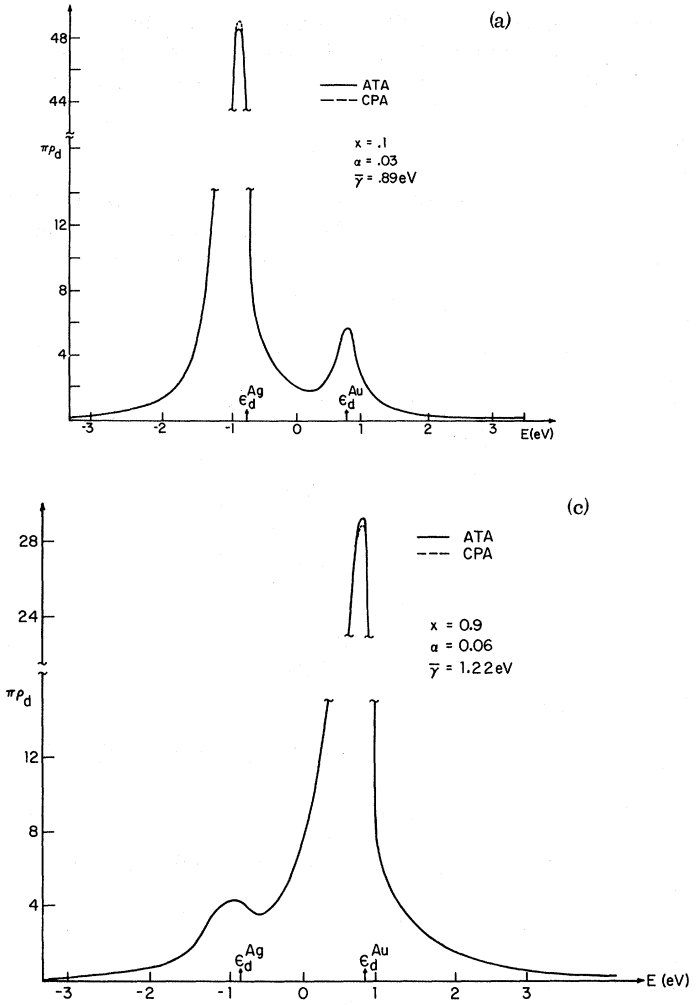

FIG. 3. Comparison of the d-band density of states calculated in the CPA and ATA for Au_xAg_{1-x}: (a) $x=0.9$, (b) $x=0.5$, and (c) $x=0.1$.

$$= xy\Delta^2 \frac{F'_{dd}(z, \bar{\epsilon}_d) - F^2_{dd}(z, \bar{\epsilon}_d)}{[1+2\bar{\epsilon}_d F_{dd}(z, \bar{\epsilon}_d)]^2} , \qquad (38)$$

where

$$F'_{dd}(z, \bar{\epsilon}_d) \equiv [dF_{dd}(z, \Sigma_d)/d\Sigma_d]_{\Sigma_d = \bar{\epsilon}_d} .$$

The ATA and CPA will agree when it can be shown that $|D(z)| \ll 1$. Suppose, for example, that z lies within the d band of the host metal. In this region $F_{dd}(z, \bar{\epsilon}_d)$ behaves like $F(z)$ for a single-band model with $w \to \alpha w_s \sim \bar{\gamma}^2/w_s$. Approximating the real and imaginary parts of F^2_{dd} and F'_{dd} by $(\alpha w_s)^{-2} \simeq (\gamma^2/w_s)^{-2}$, the magnitude of $D(z)$ is

$$|D(z)| = \frac{xy\lambda^2}{[1+(x-y)\lambda]^2 + (x-y)^2\lambda^2} , \qquad (39)$$

where $\lambda \equiv (\Delta w_s)/\bar{\gamma}^2$ is a dimensionless parameter introduced by LE. If Δ is less than the intrinsic d bandwidth $\bar{\gamma}^2/w_s$, we are in the "virtual-crystal" regime $\lambda \leq 1$, and the ATA is valid for all concentrations. However, as pointed out by LE, the range of interest for transition- and noble-metal alloys is $\lambda \sim 10$. For large values of λ, Eq. (39) shows that $|D(z)|$ is small only if $x \ll 1$. In that case

$$|D(z)| \simeq xy\lambda^2[(1-\lambda)^2 + \lambda^2]^{-1} \simeq xy \ll 1.$$

If, on the other hand, $(x-y) \sim \lambda^{-1}$ [as in Fig. 3(b)], we see that $|D(z)| \simeq xy\lambda^2 \gg 1$ and the ATA fails.

Consider now the behavior of $D(z)$ for energies in the minority d band. This is the case of greatest interest because it is within this range of energies that the results for the present model show the greatest improvement over those for the single-band model. Physically, the essential point is that the coupling of the two d subbands to the s band implies that the alloys described in Fig. 3 are not really in a split-band limit. Despite the fact that the ATA curves in Figs. 1(b) and 1(c) are qualitatively reasonable, it is nevertheless true that in the single-band model Σ^{ATA} is a very poor approximation to Σ^{CPA} for energies in the minority sub-

band. In this region (i.e., $E \simeq -\epsilon$), $F^{(0)}(z-\epsilon)$ may be approximated by $(z-\epsilon)^{-1}$ and Eq. (20) takes the form

$$\Sigma^{\mathrm{ATA}}(z) \simeq \epsilon + xy\delta^2(z+\epsilon)^{-1}. \tag{40}$$

The incorrect shape of $\rho(E)$ is in fact due to the singularity in Σ^{ATA} near $z=-\epsilon$. In the present model, the broad s band couples the two d subbands and this singularity is avoided. For $z \sim \Delta$ (and therefore $z \gg \overline{\gamma}^2/w_s$) the general equations (35) and (36) simplify to

$$F_{dd}(z, \Sigma_d) = (z-\Sigma_d)^{-1} + \overline{\gamma}^2(z-\Sigma_d)^{-2} F_s^{(0)}[z - \overline{\gamma}^2(z-\Sigma_d)^{-1}] .$$

Substitution into (38) yields

$$D(z) = \frac{xy\Delta^2\overline{\gamma}^4(z-\overline{\epsilon}_d)^{-2}[(F_s^{(0)})^2 - (F_s^{(0)})']}{[z+\overline{\epsilon}_d + 2\overline{\epsilon}_d\overline{\gamma}^2 F_s^{(0)}/(z-\overline{\epsilon}_d)]^2} . \tag{41}$$

As indicated above, $\rho_s^{(0)}(E) = -\pi^{-1}\mathrm{Im}F_s^{(0)}$ is finite throughout the minority band and the denominator in (41) never vanishes. For dilute alloys, $z-\epsilon_d \simeq -2\epsilon_d \simeq \Delta$ and (41) reduces to

$$|D(z)| \simeq xy\{[\lambda(z+\overline{\epsilon}_d)/\Delta]^2+1\}^{-1} \tag{42}$$

after approximating $\rho_s^{(0)} \sim w_s^{-1}$. If $z+\overline{\epsilon}_d > \Delta/\lambda$, the denominator in (42) is large and $|D(z)| \ll 1$. Even at the resonance energy $z=-\overline{\epsilon}_d$, $|D(z)| \simeq x \ll 1$ and the ATA is a good approximation. In the equal concentration case, Eq. (41) can be used to estimate the range of validity of the ATA. If $x=y$, $\overline{\epsilon}_d=0$ and we have

$$|D(z)| = xy\Delta^2\overline{\gamma}^4/z^4 w_s^2$$

[providing, of course, that $z > \gamma^2(w_s)$]. $|D(z)|$ is then small so long as $|z| > \gamma(xy)^{1/4}(\Delta/w_s)^{1/2}$. For Au-Ag alloys, this condition reduces to $|z| > 0.3$ eV, which is roughly the size of the region in Fig. 3(b) within which the ATA exhibits spurious behavior.

To summarize, we have shown that in dilute alloys the ATA is a good approximation over the entire range of energies. For high concentrations, the ATA fails only in a small region of energies between the two d subbands. These conclusions are valid so long as the constituent d bands lie within the broad s band of the alloy, and are therefore appropriate to a wide range of transition- and noble-metal alloys.

APPENDIX

In this appendix we demonstate the equivalence of Eqs. (23) and (17). The calculation is done most simply in a Bloch representation. If we define

$$|k\rangle = N^{-1}\textstyle\sum_n e^{i\vec{k}\cdot\vec{R}_n}|n\rangle ,$$

Eq. (23) may be rewritten as

$$\begin{aligned}\langle k|\langle T\rangle|k\rangle &= \langle t\rangle + \langle t\rangle^2 \sum_{m\neq n} e^{i\vec{k}\cdot(\vec{R}_n-\vec{R}_m)}\langle n|\tilde{G}|m\rangle \\ &\quad + \langle t\rangle^3 \sum_{m\neq n} e^{i\vec{k}\cdot(\vec{R}_n-\vec{R}_m)}\langle n|\tilde{G}|m\rangle \\ &\quad \times \sum_{p\neq m} e^{i\vec{k}\cdot(\vec{R}_m-\vec{R}_p)}\langle m|\tilde{G}|p\rangle + \cdots \\ &= \langle t\rangle + \frac{\langle t\rangle\tilde{G}'(k)\langle t\rangle}{1-\langle t\rangle\tilde{G}'(k)} ,\end{aligned} \tag{A1}$$

where

$$\begin{aligned}\tilde{G}'(k) &= \sum_{n\neq 0} e^{i\vec{k}\cdot\vec{R}_n}\langle 0|\tilde{G}|n\rangle = [z-s(k)-\sigma(z)]^{-1} - \tilde{F}(z) \\ &= \tilde{G}(k) - \tilde{F}(z) .\end{aligned} \tag{A2}$$

Substituting (A2) into (A1) and combining with the equation

$$\langle G\rangle = \tilde{G} + \tilde{G}\langle T\rangle\tilde{G} ,$$

we obtain the desired result

$$\begin{aligned}F(z) &= \sum_k \langle k|\langle G(z)\rangle|k\rangle \\ &= \sum_k\left[\tilde{G}(k) + \frac{\tilde{G}(k)\langle t\rangle\tilde{G}(k)}{1-\langle t\rangle[\tilde{G}(k)-\tilde{F}]}\right] \\ &= \sum_k \frac{\tilde{G}(k)[1+\tilde{F}\langle t\rangle]}{1-\langle t\rangle[\tilde{G}(k)-\tilde{F}]} \\ &= \sum_k\left[E-s(k)-\sigma(z)-\frac{\langle t\rangle}{1+\langle t\rangle\tilde{F}}\right]^{-1} \\ &\equiv F^{(0)}[z-\Sigma(z)] .\end{aligned}$$

*Supported in part by Grant No. GP-16504 of the National Science Foundation and the Advanced Research Projects Agency.

†Permanent address: Institut de Physique, Université de Liège, Liège, Belgium.

‡Permanent address: Moscow State University, Moscow, USSR.

[1] M. Lax, Rev. Mod. Phys. 23, 287 (1951).
[2] S. F. Edwards, Phil. Mag. 6, 617 (1961).
[3] J. L. Beeby and S. F. Edwards, Proc. Roy. Soc. (London) A274, 395 (1962).
[4] J. L. Beeby, Proc. Roy. Soc. (London) A279, 82 (1964).
[5] J. L. Beeby, Phys. Rev. 135, A130 (1964).
[6] P. Soven, Phys. Rev. 151, 539 (1966).
[7] P. Soven, Phys. Rev. 156, 809 (1967).
[8] B. Velický, S. Kirkpatrick, and H. Ehrenreich, Phys. Rev. 175, 747 (1968).
[9] P. Soven, Phys. Rev. 178, 9936 (1969).
[10] S. Kirkpatrick, B. Velický, and H. Ehrenreich, Phys. Rev. B 1, 3250 (1970).
[11] D. Stroud and H. Ehrenreich, Phys. Rev. B 2, 3197 (1970).
[12] K. Levin and H. Ehrenreich, Phys. Rev. B 3, 4172 (1971).

[13]M. Lax, Phys. Rev. 85, 621 (1952).
[14]J. Ziman, Proc. Phys. Soc. (London) 88, 387 (1966).
[15]J. L. Beeby and S. F. Edwards, Proc. Roy. Soc. (London) A274, 395 (1962).
[16]L. Schwartz and H. Ehrenreich, Ann. Phys. (N.Y.) 64, 100 (1971).
[17]See, for example, the discussion following Eq. (18) in Ref. 5. Figure 4 of this reference is also of interest.